

Strong quantum metrological limit from many-body physics

Yaoming Chu,^{1,*} Xiangbei Li,^{1,*} and Jianming Cai^{1,2,†}

¹*School of Physics, International Joint Laboratory on Quantum Sensing and Quantum Metrology,
Institute for Quantum Science and Engineering, Wuhan National High Magnetic Field Center,
Huazhong University of Science and Technology, Wuhan 430074, China*

²*Shanghai Key Laboratory of Magnetic Resonance, East China Normal University, Shanghai 200062, China*

Surpassing the standard quantum limit and even reaching the Heisenberg limit using quantum entanglement, represents the Holy Grail of quantum metrology. However, quantum entanglement is a valuable resource that does not come without a price. The exceptional overhead for the preparation of large-scale entangled states raises disconcerting concerns about whether the Heisenberg limit is fundamentally achievable. Here we find a universal speed limit set by the Lieb-Robinson light cone for the quantum Fisher information growth to characterize the metrological potential of quantum resource states during their preparation. Our main result establishes a strong precision limit of quantum metrology accounting for the complexity of many-body quantum resource state preparation and reveals a fundamental constraint for reaching the Heisenberg limit. Our result makes it possible to identify the essential features of quantum many-body systems that are crucial for achieving the quantum advantage of quantum metrology and brings a new perspective to understanding many-body quantum dynamics from quantum metrology.

Quantum metrology, as part of the rapidly rising field of quantum science and technology, is capable of achieving enhanced precision measurement by exploiting quantum strategies and promises unprecedented applications in basic science and technology [1–6]. Importantly, irrespective of classical accidental errors [1], quantum mechanics imposes a fundamental limit on the accuracy to which measurements can be performed, called the Heisenberg limit [7–9]. The celebrated Heisenberg limit conventionally refers to a measurement precision scaling as $1/N$ (where N is typically regarded as the number of probes employed) and acts as a hallmark of scaling improvement over the standard quantum limit (SQL), which arises from uncorrelated measurements and is given by $1/\sqrt{N}$. The advantage of quantum metrology in terms of reaching the Heisenberg limit often attribute to quantum entanglement [10–13], such as the “cat” state of N probes. Although the improved scaling has been unfortunately demonstrated to be fragile when suffering from noise sources [14–16], a number of clever noise-robust quantum metrological schemes [17–19] have been proposed to battle against decoherence, making it not a fundamentally unsolvable obstacle for reaching the Heisenberg limit.

In contrast, given that the preparation of large-scale entangled states of many-body quantum systems is usually a highly demanding and challenging task, the following intricate and critical problem remains elusive: whether is there any fundamental constraint that prevents reaching the Heisenberg limit imposed by the complexity of state preparation [20–22]? Addressing this problem and establishing a stronger precision limit would put comparisons of entanglement-enhanced quantum measurements with the SQL on a more fair footing, and consistently consolidate the foundation of the quantum advantage offered by quantum metrology over classical counterparts. It also relates to another crucial problem: is there any simple and universal principle to find quantum metrological systems that are favorable for achieving the quantum advantage of quantum metrology?

In this letter, we address these problems by quantifying the growth of quantum Fisher information (QFI) for the metrological state preparation in generic quantum many-body systems. As our main result, we find a universal speed limit for the QFI growth set by the celebrated Lieb-Robinson (LR) light cone from many-body physics [23, 24]. This provides a versatile tool to lower bound the minimal time required by metrological resource state preparation, and thus establishes the precision limit for quantum metrology explicitly involving the complexity of state preparation (dubbed “strong precision limit”). Applying our result to quantum many-body systems with Ising and dipolar interactions, we illustrate how to achieve the advantage of quantum metrology through long-range interacting and higher-dimensional systems, which presents insightful design principles for quantum metrological systems. The result also connects quantum metrology with quantum information propagation and offers a new perspective to understanding many-body quantum dynamics via the concept of QFI growth.

Fundamental constraint for QFI growth.— Quantum Fisher information, F_Q , as a fundamental concept in quantum metrology, determines the optimal measurement precision using a given quantum resource state ρ [25]. It quantifies the sensitivity of ρ to a parameter-dependent unitary transformation generated by an interrogation operator \mathcal{K} , i.e. $\rho_\vartheta = e^{-i\vartheta\mathcal{K}}\rho e^{i\vartheta\mathcal{K}}$ with ϑ a phase to be estimated. Usually the interrogation operator is local, $\mathcal{K} = \sum_{i=1}^N K_i$, with K_i defined on the i -th individual probe, see Fig. 1a. For a general resource state, spectrally decomposed as $\rho = \sum_n p_n |n\rangle\langle n|$, the QFI takes a structure of the following form

$$F_Q[\rho, \mathcal{K}] = 2 \sum_{n,m} \frac{(p_n - p_m)^2}{p_n + p_m} |\langle n | \mathcal{K} | m \rangle|^2, \quad (1)$$

where the sum includes only terms with $p_n + p_m > 0$. A larger QFI indicates a better distinguishability between neighboring parametrized quantum states ρ_ϑ and $\rho_{\vartheta+\delta\vartheta}$, and thus a more sensitive ρ to the operator \mathcal{K} .

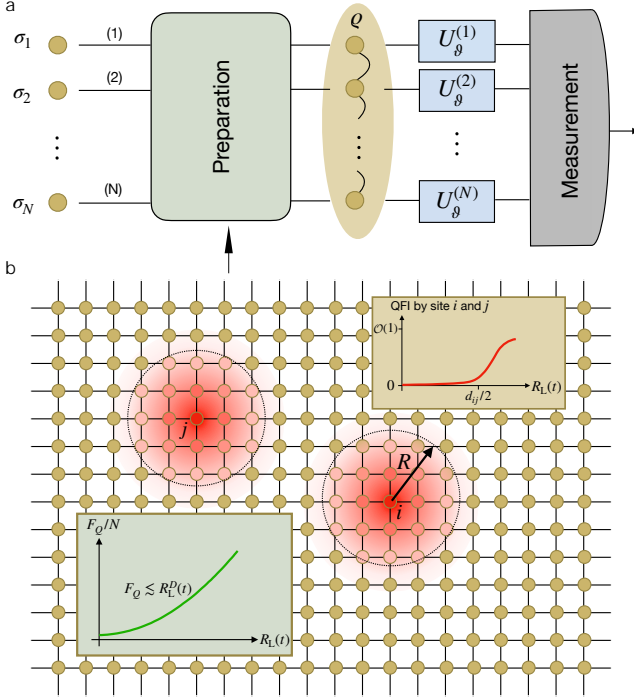


FIG. 1. **Metrological resource state preparation and QFI growth.**

a, Conventional scheme for quantum metrology. A N -probe quantum system is prepared in the resource state ρ and is fed into N parallel local channels (each one is described as $U_\theta^{(i)} \equiv e^{-i\theta K_i}$) to sense an unknown phase θ . **b**, Spreading of local operators in a quantum lattice. The quasilocality implied by LR bound ensures that $K_i(t)$ (red region) is well approximated by an operator $K_i(t, i[R])$ defined on a ball region $i[R]$ (dashed circle) with $R \gtrsim R_L(t)$, where $R_L(t)$ represents the effective light cone. The QFI collaboratively contributed by the site i and j (red curve, Sec. 1 in Supplementary Information) begins to be nonzero only when the two balls $K_i(t, i[R])$ and $K_j(t, j[R])$ grow to touch each other. Consequently, the upper bound of the QFI growth (green curve) would be constrained by the effective light cone $R_L(t)$.

Quantum metrology often seeks such metrological states ρ (e.g. GHZ state [26], squeezed spin states [27, 28], critical ground states [29], etc.) to enhance the optimal measurement precision [1]. These strongly correlated quantum metrological states are usually prepared via coherent interactions between individual probes, see e.g. [30–34]. We consider generic Hamiltonians with few-body interactions on a D -dimensional lattice, with Λ the total particle set and the cardinality $|\Lambda| = N$. In detail, the interaction Hamiltonian of a k -local form with bounded one-site energy [35] can be expressed as,

$$H = \sum_{|X| \leq k} h_X, \quad \max_{i \in \Lambda} \sum_{X: X \ni i} \|h_X\| \lesssim \mathcal{O}(1), \quad (2)$$

where each interaction term h_X acts on the particle subset $X \subset \Lambda$, and $\|\bullet\|$ is the operator norm. Remarkably, in state-of-the-art quantum platforms including trapped ions [36, 37], Bose-Einstein condensates [38–42], Rydberg atoms [43, 44]

etc., the interaction Hamiltonians to generate unprecedented levels of multipartite entanglement with $N \gtrsim \mathcal{O}(100)$ generally belong to this family of Hamiltonian [Eq. (2)].

The key is to find the speed limit of the QFI growth for a quantum metrological resource state $\rho(t)$ prepared by a unitary evolution $\mathcal{U}(t)$ with the Hamiltonian in Eq. (2), see Fig. 1a. Starting from a full product state $\sigma = \otimes_{i=1}^N \sigma_i$, the QFI of $\rho(t) = \mathcal{U}(t)\sigma\mathcal{U}^\dagger(t)$ [cf. Eq. (1)] associated with \mathcal{K} can be formulated as (Sec. 1 in Supplementary Information)

$$F_Q(t) = 2c_{\text{WY}} \sum_{i,j} \text{tr}([K_i(t), \sqrt{\sigma}]^\dagger [K_j(t), \sqrt{\sigma}]), \quad (3)$$

with $c_{\text{WY}} \in [1, 2]$ relevant to the Wigner-Yanase skew information [45], and $K_i(t) = \mathcal{U}^\dagger(t) K_i \mathcal{U}(t)$. This result reveals an explicit connection between the evolution of QFI and the spreading as well as interference of on-site operators, see Fig. 1b. Such a connection will enable us to analyze the “growth” behavior of the QFI with respect to the preparation time.

In non-relativistic quantum mechanics, by analogy to Einstein’s relativity, Lieb-Robinson bound imposes one of the most fundamental restrictions to quantum dynamics, leading to the formation of an “effective light cone”, $R_L(t)$, that bounds the propagation of quantum information to a finite velocity (i.e. causality in a quantum many-body lattice) [23]. Mathematically, the time-dependent commutator between two operators $K_i(t)$ and K_j (i.e. $[K_i(t), K_j]$) decrease rapidly with the graph-theoretic distance d_{ij} separating site i and j outside the light cone, which ensures an approximation of $K_i(t)$ as $K_i(t) \approx K_i(t, i[R])$ (Sec. 2 in Supplementary Information). Here, $R \gtrsim R_L(t)$ up to a constant factor, and $K_i(t, i[R])$ represents a projection of $K_i(t)$ onto the subset $i[R] \subset \Lambda$ that is a ball region centered at the site i with radius R , see Fig. 1b. Exploiting such a causality relation, we establish an upper bound for the growth of QFI in many-body quantum lattices as (Sec. 3 in Supplementary Information)

$$F_Q(t) \lesssim \kappa c_{\text{WY}} [1 + \gamma 2^D R_L^D(t)] N, \quad (4)$$

where $\kappa \simeq \mathcal{O}(1)$ represents the maximal spectrum width of the local interrogation operators $\{K_i\}$, and γ is a positive constant determined by the geometry of a quantum lattice. Therefore, given a state preparation time t , the maximal QFI that can be achieved is strictly constrained by the geometry and the light cone for a quantum many-body lattice. Such a fundamental constraint determines whether the metrological system can surpass the SQL and even reach the Heisenberg limit when accounting for the overhead of quantum resource state preparation.

Strong precision limit of quantum metrology.— In quantum metrology, in order to estimate a parameter λ encoded in the phase $\vartheta = \lambda\tau$ with τ the interrogation time of single measurement, the minimal uncertainty of multiple identical measurements is set via the well-known quantum Cramér-Rao bound (Sec. 4 in Supplementary Information),

$$\delta\lambda \geq N^{-\Delta/2} \lambda_{\text{SQL}} \equiv N^{-(1+\Delta)/2} \frac{1}{\sqrt{T\tau}} \quad (5)$$

Here, $\delta\lambda_{\text{SQL}} \equiv 1/\sqrt{NT}\tau$ represents the standard quantum limit with T the total measurement time. The exponent Δ characterizes the quantum metrological enhancement to beat the SQL; specifically, $\Delta = 0$ and 1 correspond to the SQL and Heisenberg scaling respectively. For a sufficiently large quantum many-body system, the preparation time (below denoted as t_p) of entangled metrological resource state would generally be much longer than the signal interrogation time (which is limited by the system's coherence time), namely $t_p \gg \tau$, and then the number of measurement repetitions is upper bounded by T/t_p . Thus, the enhancing exponent Δ is dominantly determined by the ratio of QFI to the state preparation time (Sec. 4 in Supplementary Information),

$$\Delta = \log_N \left(\frac{F_Q}{t_p} \cdot \frac{\tau}{N} \right). \quad (6)$$

Based on the QFI growth bound in Eq. (4), we are able to determine the maximal exponent Δ through the scaling behavior of (F_Q/t_p) , and then strengthen the ultimate precision limit of quantum metrology in generic quantum many-body lattices.

For short-range interacting systems, namely, the decay of interaction strength is faster than an exponential decay relative to the distance between separated sites, Lieb and Robinson proved in 1972 an effective linear light cone $R_L(t) \simeq v_{\text{LR}}t$ with $v_{\text{LR}} \sim \mathcal{O}(1)$ the so-called LR velocity [23]. By using our result in Eq. (4) that $F_Q \lesssim NR_L^D(t_p) \sim Nt_p^D$, the metrological enhancing exponent would be upper bounded by (Sec. 4 in Supplementary Information)

$$\Delta \leq 1 - \frac{1}{D}. \quad (7)$$

Particularly, for one dimensional (1D) short-range interacting quantum systems, the result implies that one can only achieve a zero enhancing exponent, i.e. $\Delta = 0$, and thereby a surprising precision scaling as $\delta\lambda_{\text{SQL}}$. In this scenario, even if the system might be able to be prepared in a global multipartite entangled state with $F_Q \sim N^2$, the Heisenberg scaling would not be feasible due to the required state preparation time that scales at least linearly with the system size, namely $t_p \sim F_Q/N \sim N$ following Eq. (4).

For long-range interacting systems, we consider two-body interactions of the form $\|h_{i,j}\| \lesssim d_{i,j}^{-\alpha}$, where $\{h_{i,j}\}$ are bipartite interaction operators, $d_{i,j}$ is the distance from the site i to j , α is the power-law decaying exponent. A strictly linear light cone exists for sufficiently large α (i.e. $\alpha > 2D + 1$) in generic long-range interacting lattices [46], and thus the quantum metrological enhancing exponent is also bounded by Eq. (7). Nevertheless, as the decaying exponent α becomes smaller, a linear light cone can be broken [47]. In the regime of $\alpha \in (2D, 2D + 1]$, the shape of the effective light cone becomes polynomial and is given by $R_L(t) \simeq ct^{1/\xi}$, where c is a constant of $\mathcal{O}(1)$ and $\xi = \alpha - 2D$ up to an arbitrarily small constant [48]. Therefore, our result in Eq. (4) leads to the following metrological enhancing exponent as (Sec. 4 in

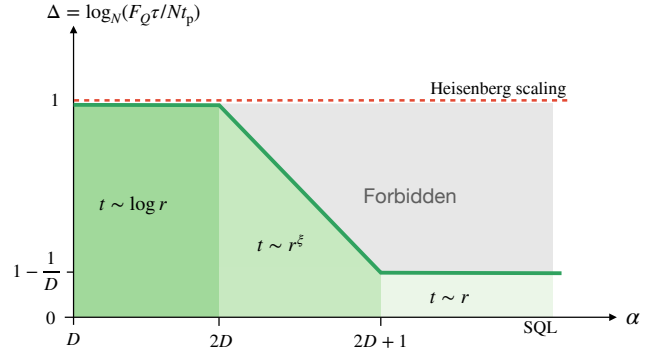


FIG. 2. **Bound of quantum metrological enhancement.** In the regime of $\alpha > 2D + 1$, a quantum many-body lattice is governed by a linear light cone ($t \sim r$), resulting in that $\Delta \leq 1 - 1/D$; while in the regime of $\alpha \leq 2D + 1$, “supersonic” information propagation (e.g. polynomial $t \sim r^\xi$ and logarithmic $t \sim \log r$ light cones) is possible, which gives rise to that $\Delta \leq 3 - \alpha/D$ for $\alpha \in (2D, 2D + 1]$ and $\Delta \leq 1 - \log_N(\text{polylog}(N))$ (i.e. approaching the Heisenberg scaling in the limit of large system size) for $\alpha \in (D, 2D]$.

Supplementary Information)

$$\Delta \leq 1 - \frac{\xi}{D}. \quad (8)$$

As one can see, as $\alpha \rightarrow 2D$ and $\xi \rightarrow 0^+$, the measurement precision would approach the Heisenberg scaling (i.e. $\Delta = 1$). While in the regime of $\alpha \in (D, 2D]$, the LR bounds give rise to a “logarithmic light cone” (i.e. $t \sim \log R$), or equivalently an exponentially growing speed of quantum information propagation [24, 48]. Similarly, according to Eq. (4), this would lead to the quantum metrological enhancement as (Sec. 4 in Supplementary Information)

$$\Delta \leq 1 - \log_N \text{polylog}(N). \quad (9)$$

Note that $\log_N \text{polylog}(N) < o(1)$ (namely, smaller than an arbitrarily small positive constant) for $N \rightarrow \infty$, therefore the Heisenberg limit becomes asymptotically achievable. In Fig. 2, we summarize the scaling behavior of these strong precision limits of quantum metrology with respect to the system size for $\alpha > D$. For *ultra* long-range interacting systems with $\alpha \in [0, D]$, the notion of quasilocality is broken [49–51]; in other words, the causal region defined by an effective light cone might disappear. In this scenario, even faster information propagation and metrological state preparation are possible. In particular, we remark that the interaction regime of $\alpha = 0$ offers very favorable systems to prepare many-body entangled metrological resource states, especially in experimental platforms of Bose-Einstein condensates [13, 38–40, 42].

Design principles for quantum metrological systems.— Our result suggests that long-range interaction is favorable for achieving the quantum advantage of quantum metrology over the SQL. Below we present an illustrative example of the Ising

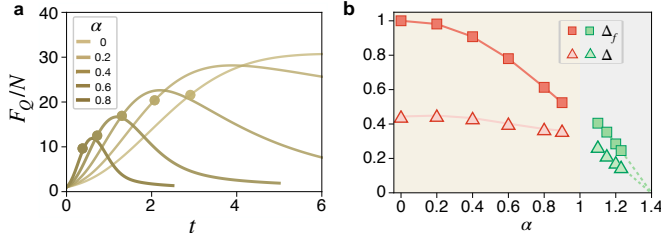


FIG. 3. **Metrological enhancement by Ising chain with long-range interaction.** **a**, QFI growth with respect to the evolution time for different values of α with $N = 60$ sites. Starting from the coherent spin state along the x direction, we maximize the QFI at all times t by optimizing local interrogation operators, $K_i = S_{\hat{n}_i}$, with $S_{\hat{n}}$ the spin-1/2 operator along the direction \hat{n} . The circles mark the optimum of (F_Q/t_p) for $t_p > 0$. **b**, Metrological enhancing exponent $\{\Delta_f = \log_N(F_Q/N), \Delta = \log_N(F_Q\tau/Nt_p)\}$ for different values of α . We obtain each value of Δ and Δ_f by numerically fitting the quantities (F_Q/t_p) and F_Q with respect to the system size N (Sec. 5 in Supplementary Information). Here, the interrogation time is set as a unit ($\tau = 1$).

chain ($D = 1$) with the Hamiltonian given by

$$H_{\text{Ising}} = \frac{1}{N_\alpha} \sum_{i < j} \frac{4}{|i - j|^\alpha} S_i^z S_j^z, \quad (10)$$

where S_i represents the spin-1/2 operator associated with the site i , and N_α is a normalization factor chosen as $N^{1-\alpha}$ for $\alpha \in [0, 1)$, and 1 for $\alpha > 1$ respectively to ensure system energy an extensive quantity [52]. Despite the fact that all terms of the Ising Hamiltonian commute, rich genuine quantum features (e.g. spin squeezing [27], quantum magnetism [36] etc.) can occur. In Fig. 3a, we investigate in detail the growth dynamics of the QFI for different values of α , and find the maximal point where an optimal enhancing factor (F_Q/t_p) [cf. Eq.(6)] is obtained. It is worth noting that the optimal metrological points are no more those maximizing the QFI when taking the state preparation time into account. As can be seen from Fig. 3b, for long-range interaction, the metrological enhancing exponents Δ are smaller than the ones (denoted as Δ_f) without considering the required time for resource state preparation (i.e. solely determined by F_Q/N), namely $\Delta < \Delta_f \equiv \log_N(F_Q/N)$. Nevertheless, it still results in an apparent quantum advantage over the SQL (i.e. $\Delta \gtrsim 0.4$) if $\alpha < 1$. In contrast, the SQL can not be surpassed for $\alpha \gtrsim 1.4$, since the maximal QFI would only scale approximately as $F_Q \sim N$ (cf. Sec. 5 and Fig. S1 in Supplementary Information).

Our result also hints that the quantum advantage of quantum metrology can be achieved by exploiting higher-dimensional systems. For a larger dimension D , local information can propagate along more directions to spread across the entire lattice, resulting in the speed-up of QFI growth which is evidenced by the power exponent D of $R_L(t)$ [cf. Eq. (4)]. Given a power-law decaying exponent α , a larger D would change the shape of the effective light cone, and result in an improved bound for the strong precision limit (see

Fig. 2). An important example is the multipartite entanglement generation in quantum systems with $U(1)$ symmetric dipolar interactions, i.e. $H_{XX} = -\sum_{i < j} (S_i^x S_j^x + S_i^y S_j^y) / d_{ij}^3$. This type of dipolar system can be prominently engineered in dipolar molecules [53], solid-state spin ensembles [54, 55], Rydberg-atom arrays [43], etc. In the 1D case, the linear light cone (i.e. $\alpha = 3 \geq 2D + 1$ with $D = 1$) prevents the advantage of quantum metrology (namely $\Delta = 0$) due to the overhead for the state preparation time. When we extend to the higher-dimensional system (e.g. $D = 2$), α would fall into the regime of $(D, 2D)$, and the linear light cone fails to hold, which would make it possible to surpass the SQL according to our result. This is verified by the fact that the one-axis-twisting-like dynamics in such a planar dipolar array can generate spin-squeezed states with squeezing parameter $\xi_R^2 \sim N^{-2/3}$ (and thus $F_Q \gtrsim N^{5/3}$) at an evolution time scaling as $t \sim N^{1/3}$ [56]. It indicates a metrological enhancing exponent $\Delta \gtrsim 1/3$ over the SQL. By further engineering the forms of long-range interactions (e.g. by designing quantum gate sequences etc.) of a given power-law decaying exponent α , the preparation time for metrological resource states (e.g. GHZ-like states with $F_Q \simeq N^2$) can scale as $t_p \lesssim \text{polylog}(N)$ for $\alpha \in (D, 2D)$ [47], which leads to a metrological enhancing exponent of $\Delta = 1 - \log_N \text{polylog}(N)$. The result achieves the asymptotic Heisenberg limit up to subalgebraic corrections [48], and thus confirms the strong precision limit in Eq. (9).

Conclusion & prospects.— To summarize, we reveal a connection between Lieb-Robinson light cone and quantum metrology, and present a fundamental constraint for the QFI growth in generic quantum many-body lattices. This bound allows us to establish strong precision limits for quantum metrology that include the overhead of quantum resource state preparation over conventional precision limits. A remaining complementary aspect would be taking the readout process into account as well, which is expected to even tighten the present scaling behavior. The result allows us to identify the crucial features of quantum many-body systems for entanglement-enhanced quantum metrology, and thus provides guiding principles for the design of many-body quantum metrological systems.

The established general bound of QFI growth [cf. Eq. (4)] would also provide interesting insights into many-body quantum dynamics. For example, considering the GHZ state preparation through adiabatic strategy from the paramagnetic phase of a transverse field Ising chain (namely with an initial state of coherent spin state), we can immediately conclude that the minimal evolution time of at least $t \simeq \mathcal{O}(F_Q/v_{\text{LR}}N) \sim \mathcal{O}(N)$ is required according to the present bound of QFI growth. This is consistent with $\mathcal{O}(N^z)$ given by the adiabatic theorem (here z represents the dynamical critical exponent and $z = 1$ in this case) [57]. More generally, our result predicts that, by starting from a full product state and engineering short-range interactions in a 1D lattice, the minimal time to prepare a metrologically useful, k -partite entangled state (i.e. $F_Q/N \geq k$ [58]) would be lower bounded by $t \gtrsim k/v_{\text{LR}}$.

Our result can be extended to dynamical quantum metrological frameworks [21, 59], where the parameter information is encoded via a dynamical evolution governed by a Hamiltonian of the form, $\mathcal{H} = H + \lambda K$, with H given by Eq. (2). In this framework, the corresponding time-evolved local operator $K_i(t)$ in Eq. (3) would be generalized by the time average $\bar{K}_i(\tau) = \int_0^\tau K_i(s) ds$ over a single run of interrogation and then the QFI growth would be bounded by the effective light cone as $F_Q/N \lesssim \int_0^\tau dt_1 \int_0^\tau dt_2 [R_L(t_1) + R_L(t_2)]^D$. For 1D short-range interacting systems with $R_L(t) \sim t$, this integral would yield that $F_Q \lesssim N\tau^3$, which implies that achieving the Heisenberg limit via dynamical quantum metrological frameworks would require the interrogation time $\tau \gtrsim \mathcal{O}(N)$. This result then further sets conditions for the system's coherence time in order to reach the Heisenberg limit.

Acknowledgements.— We thank Lijian Zhang for helpful discussions. The work is supported by the National Natural Science Foundation of China (12161141011, 11874024), the National Key R&D Program of China (2018YFA0306600), the Interdisciplinary Program of the Wuhan National High Magnetic Field Center (WHMFC202106), and Shanghai Key Laboratory of Magnetic Resonance (East China Normal University).

* These authors contributed equally.

† jianmingcai@hust.edu.cn

- [1] V. Giovannetti, S. Lloyd, and L. Maccone, Advances in quantum metrology, *Nat. Photon.* **5**, 222 (2011).
- [2] M. G. A. Paris, Quantum estimation for quantum technology, *Int. J. Quantum. Inform.* **10.1142/S0219749909004839** (2011).
- [3] C. L. Degen, F. Reinhard, and P. Cappellaro, Quantum sensing, *Rev. Mod. Phys.* **89**, 035002 (2017).
- [4] D. Budker and M. Romalis, Optical magnetometry, *Nat. Phys.* **3**, 227 (2007).
- [5] J. Aasi et al., Enhanced sensitivity of the LIGO gravitational wave detector by using squeezed states of light, *Nat. Photon.* **7**, 613 (2013).
- [6] K. M. Backes, D. A. Palken, S. A. Kenany, B. M. Brubaker, S. B. Cahn, A. Droster, G. C. Hilton, S. Ghosh, H. Jackson, S. K. Lamoreaux, A. F. Leder, K. W. Lehnert, S. M. Lewis, M. Malnou, R. H. Maruyama, N. M. Rapis, M. Simanovskaia, S. Singh, D. H. Speller, I. Urdinaran, L. R. Vale, E. C. van Asendelft, K. van Bibber, and H. Wang, A quantum enhanced search for dark matter axions, *Nature* **590**, 238 (2021).
- [7] V. Giovannetti, Quantum-enhanced measurements: Beating the standard quantum limit, *Science* **306**, 1330 (2004).
- [8] S. Boixo, S. T. Flammia, C. M. Caves, and J. Geremia, Generalized limits for single-parameter quantum estimation, *Phys. Rev. Lett.* **98**, 090401 (2007).
- [9] W. Górecki, R. Demkowicz-Dobrzański, H. M. Wiseman, and D. W. Berry, π -corrected Heisenberg limit, *Phys. Rev. Lett.* **124**, 030501 (2020).
- [10] G. Tóth and I. Apellaniz, Quantum metrology from a quantum information science perspective, *J. Phys. A* **47**, 424006 (2014).
- [11] T. Nagata, R. Okamoto, J. L. O'Brien, K. Sasaki, and S. Takeuchi, Beating the standard quantum limit with four-entangled photons, *Science* **316**, 726 (2007).
- [12] L. Pezzè, A. Smerzi, M. K. Oberthaler, R. Schmied, and P. Treutlein, Quantum metrology with nonclassical states of atomic ensembles, *Rev. Mod. Phys.* **90**, 035005 (2018).
- [13] G. P. Greve, C. Luo, B. Wu, and J. K. Thompson, Entanglement-enhanced matter-wave interferometry in a high-finesse cavity, *Nature* **610**, 472 (2022).
- [14] S. F. Huelga, C. Macchiavello, T. Pellizzari, A. K. Ekert, M. B. Plenio, and J. I. Cirac, Improvement of frequency standards with quantum entanglement, *Phys. Rev. Lett.* **79**, 3865 (1997).
- [15] B. M. Escher, R. L. de Matos Filho, and L. Davidovich, General framework for estimating the ultimate precision limit in noisy quantum-enhanced metrology, *Nat. Phys.* **7**, 406 (2011).
- [16] R. Demkowicz-Dobrzański, J. Kołodyński, and M. Guţă, The elusive Heisenberg limit in quantum-enhanced metrology, *Nat. Commun.* **3**, 1063 (2012).
- [17] E. M. Kessler, I. Lovchinsky, A. O. Sushkov, and M. D. Lukin, Quantum error correction for metrology, *Phys. Rev. Lett.* **112**, 150802 (2014).
- [18] G. Arrad, Y. Vinkler, D. Aharonov, and A. Retzker, Increasing sensing resolution with error correction, *Phys. Rev. Lett.* **112**, 150801 (2014).
- [19] S. Zhou, M. Zhang, J. Preskill, and L. Jiang, Achieving the Heisenberg limit in quantum metrology using quantum error correction, *Nat. Commun.* **9**, 78 (2018).
- [20] S. Dooley, W. J. Munro, and K. Nemoto, Quantum metrology including state preparation and readout times, *Phys. Rev. A* **94**, 052320 (2016).
- [21] A. J. Hayes, S. Dooley, W. J. Munro, K. Nemoto, and J. Dunningham, Making the most of time in quantum metrology: concurrent state preparation and sensing, *Quantum Sci. Technol.* **3**, 035007 (2018).
- [22] L. P. McGuinness, The case against entanglement improved measurement precision, *arXiv:2112.04354* (2021).
- [23] E. H. Lieb and D. W. Robinson, The finite group velocity of quantum spin systems, *Commun. Math. Phys.* **28**, 251 (1972).
- [24] M. B. Hastings and T. Koma, Spectral gap and exponential decay of correlations, *Commun. Math. Phys.* **265**, 781 (2006).
- [25] S. L. Braunstein and C. M. Caves, Statistical distance and the geometry of quantum states, *Phys. Rev. Lett.* **72**, 3439 (1994).
- [26] D. Leibfried, M. D. Barrett, T. Schaetz, J. Britton, J. Chiaverini, W. M. Itano, J. D. Jost, C. Langer, and D. J. Wineland, Toward Heisenberg-limited spectroscopy with multiparticle entangled states, *Science* **304**, 1476 (2004).
- [27] M. Kitagawa and M. Ueda, Squeezed spin states, *Phys. Rev. A* **47**, 5138 (1993).
- [28] H. Bao, J. Duan, S. Jin, X. Lu, P. Li, W. Qu, M. Wang, I. Novikova, E. E. Mikhailov, K.-F. Zhao, K. Mølmer, H. Shen, and Y. Xiao, Spin squeezing of 10^{11} atoms by prediction and retrodiction measurements, *Nature* **581**, 159 (2020).
- [29] I. Frérôt and T. Roscilde, Quantum critical metrology, *Phys. Rev. Lett.* **121**, 020402 (2018).
- [30] H. Strobel, W. Muessel, D. Linnemann, T. Zibold, D. B. Hume, L. Pezzè, A. Smerzi, and M. K. Oberthaler, Fisher information and entanglement of non-Gaussian spin states, *Science* **345**, 424 (2014).
- [31] C. Song, K. Xu, H. Li, Y.-R. Zhang, X. Zhang, W. Liu, Q. Guo, Z. Wang, W. Ren, J. Hao, H. Feng, H. Fan, D. Zheng, D.-W. Wang, H. Wang, and S.-Y. Zhu, Generation of multicomponent atomic Schrödinger cat states of up to 20 qubits, *Science* **365**, 574 (2019).
- [32] Q. Liu, L.-N. Wu, J.-H. Cao, T.-W. Mao, X.-W. Li, S.-F. Guo, M. K. Tey, and L. You, Nonlinear interferometry beyond classical limit enabled by cyclic dynamics, *Nat. Phys.* **18**, 167 (2022).
- [33] C. D. Marciniak, T. Feldker, I. Pogorelov, R. Kaubruegger,

- D. V. Vasilyev, R. van Bijnen, P. Schindler, P. Zoller, R. Blatt, and T. Monz, Optimal metrology with programmable quantum sensors, *Nature* **603**, 604 (2022).
- [34] T. M. Graham, Y. Song, J. Scott, C. Poole, L. Phuttitarn, K. Jooya, P. Eichler, X. Jiang, A. Marra, B. Grinkemeyer, M. Kwon, M. Ebert, J. Cherek, M. T. Lichtman, M. Gillette, J. Gilbert, D. Bowman, T. Ballance, C. Campbell, E. D. Dahl, O. Crawford, N. S. Blunt, B. Rogers, T. Noel, and M. Saffman, Multi-qubit entanglement and algorithms on a neutral-atom quantum computer, *Nature* **604**, 457 (2022).
- [35] T. Kuwahara and K. Saito, Exponential clustering of bipartite quantum entanglement at arbitrary temperatures, *Phys. Rev. X* **12**, 021022 (2022).
- [36] J. W. Britton, B. C. Sawyer, A. C. Keith, C.-C. J. Wang, J. K. Freericks, H. Uys, M. J. Biercuk, and J. J. Bollinger, Engineered two-dimensional Ising interactions in a trapped-ion quantum simulator with hundreds of spins, *Nature* **484**, 489 (2012).
- [37] J. G. Bohnet, B. C. Sawyer, J. W. Britton, M. L. Wall, A. M. Rey, M. Foss-Feig, and J. J. Bollinger, Quantum spin dynamics and entanglement generation with hundreds of trapped ions, *Science* **352**, 1297 (2016).
- [38] C. Gross, T. Zibold, E. Nicklas, J. Estève, and M. K. Oberthaler, Nonlinear atom interferometer surpasses classical precision limit, *Nature* **464**, 1165 (2010).
- [39] M. F. Riedel, P. Böhi, Y. Li, T. W. Hänsch, A. Sinatra, and P. Treutlein, Atom-chip-based generation of entanglement for quantum metrology, *Nature* **464**, 1170 (2010).
- [40] W. Muessel, H. Strobel, D. Linnemann, D. B. Hume, and M. K. Oberthaler, Scalable spin squeezing for quantum-enhanced magnetometry with Bose-Einstein condensates, *Phys. Rev. Lett.* **113**, 103004 (2014).
- [41] X.-Y. Luo, Y.-Q. Zou, L.-N. Wu, Q. Liu, M.-F. Han, M. K. Tey, and L. You, Deterministic entanglement generation from driving through quantum phase transitions, *Science* **355**, 620 (2017).
- [42] S. Colombo, E. Pedrozo-Peñafiel, A. F. Adiyatullin, Z. Li, E. Mendez, C. Shu, and V. Vuletić, Time-reversal-based quantum metrology with many-body entangled states, *Nat. Phys.* **18**, 925 (2022).
- [43] A. Browaeys and T. Lahaye, Many-body physics with individually controlled Rydberg atoms, *Nat. Phys.* **16**, 132 (2020).
- [44] S. Ebadi, T. T. Wang, H. Levine, A. Keesling, G. Semeghini, A. Omran, D. Bluvstein, R. Samajdar, H. Pichler, W. W. Ho, S. Choi, S. Sachdev, M. Greiner, V. Vuletić, and M. D. Lukin, Quantum phases of matter on a 256-atom programmable quantum simulator, *Nature* **595**, 227 (2021).
- [45] S. Luo, Wigner-Yanase skew information vs. quantum Fisher information, *Proc. Am. Math. Soc.* **132**, 885 (2004).
- [46] T. Kuwahara and K. Saito, Strictly linear light cones in long-range interacting systems of arbitrary dimensions, *Phys. Rev. X* **10**, 031010 (2020).
- [47] M. C. Tran, A. Y. Guo, A. Deshpande, A. Lucas, and A. V. Gorshkov, Optimal state transfer and entanglement generation in power-law interacting systems, *Phys. Rev. X* **11**, 031016 (2021).
- [48] M. C. Tran, A. Y. Guo, C. L. Baldwin, A. Ehrenberg, A. V. Gorshkov, and A. Lucas, Lieb-Robinson light cone for power-law interactions, *Phys. Rev. Lett.* **127**, 160401 (2021).
- [49] J. Eisert, M. van den Worm, S. R. Manmana, and M. Kastner, Breakdown of quasilocality in long-range quantum lattice models, *Phys. Rev. Lett.* **111**, 260401 (2013).
- [50] P. Hauke and L. Tagliacozzo, Spread of correlations in long-range interacting quantum systems, *Phys. Rev. Lett.* **111**, 207202 (2013).
- [51] P. Richerme, Z.-X. Gong, A. Lee, C. Senko, J. Smith, M. Foss-Feig, S. Michalakis, A. V. Gorshkov, and C. Monroe, Non-local propagation of correlations in quantum systems with long-range interactions, *Nature* **511**, 198 (2014).
- [52] A. Y. Guo, M. C. Tran, A. M. Childs, A. V. Gorshkov, and Z.-X. Gong, Signaling and scrambling with strongly long-range interactions, *Phys. Rev. A* **102**, 010401 (2020).
- [53] S. A. Moses, J. P. Covey, M. T. Miecnikowski, D. S. Jin, and J. Ye, New frontiers for quantum gases of polar molecules, *Nat. Phys.* **13**, 13 (2017).
- [54] S. Choi, N. Y. Yao, and M. D. Lukin, Quantum metrology based on strongly correlated matter, arXiv:1801.00042 [10.48550/arXiv.1801.00042](https://arxiv.org/abs/1801.00042) (2017).
- [55] T.-X. Zheng, A. Li, J. Rosen, S. Zhou, M. Koppenhöfer, Z. Ma, F. T. Chong, A. A. Clerk, L. Jiang, and P. C. Maurer, Preparation of metrological states in dipolar-interacting spin systems, *npj Quantum Inf.* **8**, 1 (2022).
- [56] T. Comparin, F. Mezzacapo, and T. Roscilde, Multipartite entangled states in dipolar quantum simulators, *Phys. Rev. Lett.* **129**, 150503 (2022).
- [57] M. M. Rams, P. Sierant, O. Dutta, P. Horodecki, and J. Zakrzewski, At the limits of criticality-based quantum metrology: Apparent super-Heisenberg scaling revisited, *Phys. Rev. X* **8**, 021022 (2018).
- [58] P. Hauke, M. Heyl, L. Tagliacozzo, and P. Zoller, Measuring multipartite entanglement through dynamic susceptibilities, *Nat. Phys.* **12**, 778 (2016).
- [59] Y. Chu, S. Zhang, B. Yu, and J. Cai, Dynamic framework for criticality-enhanced quantum sensing, *Phys. Rev. Lett.* **126**, 010502 (2021).

Supplementary Information

CONTENTS

1. Connection between QFI growth and local operator spreading	2
2. Causality relation for local operator spreading	4
3. Proof of the bound for QFI growth	5
4. Proof of the strong precision limit of quantum metrology	7
5. Behavior of the QFI growth of Ising model	9
References	11

1. Connection between QFI growth and local operator spreading

By noticing that

$$p_n + p_m \leq (\sqrt{p_n} + \sqrt{p_m})^2 \leq 2(p_n + p_m), \quad (\text{S1})$$

for $p_n > 0$ and $p_m > 0$, one can find that

$$(\sqrt{p_n} - \sqrt{p_m})^2 \leq \frac{(p_n - p_m)^2}{p_n + p_m} \leq 2(\sqrt{p_n} - \sqrt{p_m})^2. \quad (\text{S2})$$

Based on the definition of QFI in Eq. (1) in the main text, we have

$$2 \sum_{n,m} (\sqrt{p_n} - \sqrt{p_m})^2 |\langle n | \mathcal{K} | m \rangle|^2 \leq F_Q[\varrho, \mathcal{K}] \leq 4 \sum_{n,m} (\sqrt{p_n} - \sqrt{p_m})^2 |\langle n | \mathcal{K} | m \rangle|^2. \quad (\text{S3})$$

By further introducing a coefficient $c_{\text{WY}} \in [1, 2]$, the following expression for the QFI can be obtained,

$$F_Q[\varrho, \mathcal{K}] = 2c_{\text{WY}} \sum_{n,m} (\sqrt{p_n} - \sqrt{p_m})^2 |\langle n | \mathcal{K} | m \rangle|^2. \quad (\text{S4})$$

Therefore, the QFI of the prepared metrological state $\varrho(t)$ at an evolution time t can be formulated as

$$\begin{aligned} F_Q[\varrho(t), \mathcal{K}] &= 2c_{\text{WY}} \sum_{n,m} (\sqrt{p_n} - \sqrt{p_m})^2 |\langle n | \mathcal{K} | m \rangle|^2 \\ &= 2c_{\text{WY}} \sum_{n,m} \langle n | [\mathcal{K}, \sqrt{\varrho(t)}]^\dagger | m \rangle \langle m | [\mathcal{K}, \sqrt{\varrho(t)}] | n \rangle \\ &= 2c_{\text{WY}} \text{tr} \left([\mathcal{K}, \sqrt{\varrho(t)}]^\dagger [\mathcal{K}, \sqrt{\varrho(t)}] \right) \\ &= 2c_{\text{WY}} \text{tr} \left([\mathcal{K}(t), \sqrt{\sigma}]^\dagger [\mathcal{K}(t), \sqrt{\sigma}] \right) \\ &= 2c_{\text{WY}} \sum_{i,j} \text{tr} \left([K_i(t), \sqrt{\sigma}]^\dagger [K_j(t), \sqrt{\sigma}] \right), \end{aligned} \quad (\text{S5})$$

Here, the interrogation operator is $\mathcal{K}(t) = \mathcal{U}^\dagger(t)\mathcal{K}\mathcal{U}(t) = \sum_i K_i(t)$, where $K_i(t) \equiv \mathcal{U}^\dagger(t)K_i\mathcal{U}(t)$ represents the time evolution of local interrogation operators in the Heisenberg picture. The last equality [namely Eq. (3) in the main text] implies that the QFI dynamics to prepare a metrological resource state is deeply related to the spreading of local operators. We define the component of the QFI collaboratively contributed by the site i and j as

$$\alpha_{ij}(t) \equiv \text{tr} \left([K_i(t), \sqrt{\sigma}]^\dagger [K_j(t), \sqrt{\sigma}] \right), \quad (\text{S6})$$

and the QFI can then be written as

$$F_Q[\varrho(t), \mathcal{K}] = 2c_{\text{WY}} \sum_{i,j} \alpha_{ij}(t). \quad (\text{S7})$$

Generally, by utilizing Cauchy–Schwarz inequality, we obtain that

$$\begin{aligned} |\alpha_{ij}(t)|^2 &\leq \text{tr} \left([K_i(t), \sqrt{\sigma}]^\dagger [K_i(t), \sqrt{\sigma}] \right) \text{tr} \left([K_j(t), \sqrt{\sigma}]^\dagger [K_j(t), \sqrt{\sigma}] \right) \\ &\leq \frac{1}{4} F_Q[\varrho, K_i] F_Q[\varrho, K_j] \\ &\leq \frac{1}{4} \|K_i\|_s^2 \|K_j\|_s^2. \end{aligned} \quad (\text{S8})$$

The second inequality results from a similar relation as Eq. (S5) between the QFI and the local operator K_i , namely

$$F_Q[\varrho(t), K_i] = 2c_{\text{WY}} \text{tr} \left([K_i(t), \sqrt{\sigma}]^\dagger [K_i(t), \sqrt{\sigma}] \right) = 2c_{\text{WY}} \alpha_{ii}(t), \quad (\text{S9})$$

which directly yields that

$$\alpha_{ii}(t) \leq \frac{1}{2} F_Q[\varrho(t), K_i]. \quad (\text{S10})$$

While in the third inequality, we use the fact that $F_Q[\varrho, K_i] \leq \|K_i\|_s^2$ (cf. Ref. [S1]), with the semi-norm $\|\bullet\|_s$ taking the spectrum width, namely the

difference between the largest and smallest eigenvalues. By further defining $\kappa \equiv \max_{i \in \Lambda} \|K_i\|_s^2$ as the maximum spectrum width of the local interrogation operators $\{K_i\}$, we conclude that $|\alpha_{ij}(t)| \leq \kappa/2 \sim \mathcal{O}(1)$ for arbitrary i and j .

2. Causality relation for local operator spreading

In this section, we sketch the proof for the projection of the time-evolved local operator [subject to the Hamiltonian in Eq. (2) of the main text], $K_i(t) = \mathcal{U}^\dagger(t) K_i \mathcal{U}(t)$. Mathematically, we define the projection operation onto its neighboring ball region denoted by $i[R]$ as

$$K_i(t, i[R]) \equiv \frac{1}{\text{tr}_{i[R]^c} \hat{\mathbb{1}}_{i[R]^c}} \text{tr}_{i[R]^c} [K_i(t)] \otimes \hat{\mathbb{1}}_{i[R]^c}, \quad (\text{S11})$$

where $i[R]^c$ denotes the complementary set of $i[R]$, i.e. $i[R]^c = \Lambda \setminus i[R]$. Following Ref. [S2], let U be a unitary operator acting on $i[R]^c$ and $\mu(U)$ be the Haar measure for U , one can rewrite $K_i(t, i[R])$ in the following form

$$K_i(t, i[R]) = \int d\mu(U) U K_i(t) U^\dagger, \quad (\text{S12})$$

and therefore

$$\|K_i(t) - K_i(t, i[R])\| \leq \int d\mu(U) \|[K_i(t), U]\| \leq \max_U \|[K_i(t), U]\|, \quad (\text{S13})$$

where \max_U accepts all unitary operators U supported on $i[R]^c$. By further using the standard commutator form of Lieb-Robinson bound for generic quantum many-body lattices, one can find that

$$\|K_i(t) - K_i(t, i[R])\| \leq \max_U \|[K_i(t), U]\| \leq C(t, R). \quad (\text{S14})$$

Here, $C(t, R)$ is a function that takes the forms of: (i) $C(t, R) \sim e^{vt-R}$ and $v \simeq \mathcal{O}(1)$ for short-range interaction [S3]; (ii) $C(t, R) \sim t^a/R^b$ (with $a, b \simeq \mathcal{O}(1)$)

are positive exponents) for long-range interactions with $\alpha > 2D$ [S4]; and (iii) $C(t, R) \sim e^{vt}/R^\alpha$ and $v \simeq \mathcal{O}(1)$ for long-range interactions with $\alpha \in (D, 2D]$ [S5]. The right-hand side of Eq. (S14) would decay to zero by requiring that $R \gtrsim R_L(t)$ (up to a constant factor), where $R_L(t)$ represents the effective light cone. In this sense [S6], one obtains that

$$K_i(t) \simeq K_i(t, i[R]) \quad \text{if} \quad R \gtrsim R_L(t), \quad (\text{S15})$$

and below we further abbreviate it as $K_{i[R]}(t) \equiv K_i(t, i[R])$ for simplicity.

3. Proof of the bound for QFI growth

Based on the causality relation in the above section, the component of the QFI collaboratively contributed by the site i and j can be approximately rewritten as

$$\alpha_{ij}(t) \simeq \text{tr} \left([K_{i[R]}(t), \sqrt{\sigma}]^\dagger [K_{j[R]}(t), \sqrt{\sigma}] \right) \quad \text{if} \quad R \gtrsim R_L(t). \quad (\text{S16})$$

Importantly, if the distance between the site i and j is outside the light cone, i.e. $d_{ij} \geq 2R \gtrsim 2R_L(t)$, the two ball regions $K_{i[R]}(t)$ and $K_{j[R]}(t)$ would fail to intersect with each other (see Fig. 1b in the main text), and one can derive that

$$\begin{aligned} \alpha_{ij}(t) &= \text{tr} \left(\sqrt{\sigma_{\Lambda \setminus i[R]}} [K_{i[R]}(t), \sqrt{\sigma_{i[R]}}]^\dagger [K_{j[R]}(t), \sqrt{\sigma_{j[R]}}] \sqrt{\sigma_{\Lambda \setminus j[R]}} \right) \\ &= \text{tr} \left(\sqrt{\sigma_{i[R]}} [K_{i[R]}(t), \sqrt{\sigma_{i[R]}}]^\dagger [K_{j[R]}(t), \sqrt{\sigma_{j[R]}}] \sqrt{\sigma_{j[R]}} \sigma_{\Lambda \setminus (i[R] \cup j[R])} \right) \\ &= \text{tr} \left(\sqrt{\sigma_{i[R]}} [K_{i[R]}(t), \sqrt{\sigma_{i[R]}}]^\dagger \right) \text{tr} \left([K_{j[R]}(t), \sqrt{\sigma_{j[R]}}] \sqrt{\sigma_{j[R]}} \right) \\ &= 0, \end{aligned} \quad (\text{S17})$$

where σ_A denotes the projection of σ onto the region $A \subset \Lambda$. The second equality results from that

$$\sqrt{\sigma_{\Lambda \setminus i[R]}} \sqrt{\sigma_{\Lambda \setminus j[R]}} = \sqrt{\sigma_{i[R]}} \sqrt{\sigma_{j[R]}} \sigma_{\Lambda \setminus (i[R] \cup j[R])}, \quad (\text{S18})$$

due to the non-intersection of the two sets $i[R]$ and $j[R]$. The fourth equality in Eq. (S17) can be obtained by noticing the identity that $\text{tr}([A, B]B) = 0$ with A and B arbitrary Hermitian operators. Consequently, the QFI (Eq.S7) can be bounded as

$$\begin{aligned} F_Q &= 2c_{\text{WY}} \sum_i \left[\alpha_{ii}(t) + \beta_i(t) \sum_{j \in i[2R] \setminus i} 1 \right] \\ &\leq 2c_{\text{WY}} \sum_i [\alpha_{ii}(t) + \beta_i(t) \gamma 2^D R^D] \end{aligned} \quad (\text{S19})$$

with $\beta_i(t) \equiv \sum_{j \in i[2R] \setminus i} \text{Re}[\alpha_{ij}(t)] / \sum_{j \in i[2R] \setminus i} 1 \leq \kappa/2$. In the second inequality of Eq. (S19), we have used a geometry assumption that $\max_{i \in \Lambda} |i[R]| \leq \gamma R^D$, where the introduced geometric parameter γ is determined based on the lattice structure alone. By further defining that $\alpha_t \equiv \max_{i \in \Lambda} \alpha_{ii}(t)$ as well as $\beta_t \equiv \max_{i \in \Lambda} \beta_i(t)$, and taking $R = R_L(t)$, we arrive at

$$F_Q \lesssim 2c_{\text{WY}} [\alpha_t + \beta_t 2^D \gamma R_L^D(t)] N. \quad (\text{S20})$$

This result straightforwardly gives rise to Eq.(4) in the main text using $\{|\alpha_t|, |\beta_t|\} \leq \kappa/2$.

4. Proof of the strong precision limit of quantum metrology

The celebrated quantum Cramér-Rao bound [S7] states that the ultimate measurement precision via local unbiased estimates is lower bounded by

$$\delta\lambda \geq \frac{1}{\sqrt{\nu F_Q \tau^2}}, \quad (\text{S21})$$

where ν is the number of identical measurement repetitions and is constrained by the total measurement time T , i.e. $\nu \leq T/(\tau + t_p)$. Here, t_p and τ represent the required time for single-run metrological state preparation and signal interrogation respectively. As a result, the above precision limit can be reformulated as

$$\delta\lambda \geq \sqrt{\frac{N(1 + t_p/\tau)}{F_Q}} \delta\lambda_{\text{SQL}} \equiv N^{-\frac{\Delta}{2}} \delta\lambda_{\text{SQL}}, \quad (\text{S22})$$

where $\delta\lambda_{\text{SQL}} \equiv 1/\sqrt{NT\tau}$ represents the standard quantum limit (SQL). By making the natural assumption that $t_p \gg \tau$ for large many-body quantum systems, one would obtain Eq. (5) with the metrological enhancing exponent [Eq. (6) in the main text] defined as

$$\Delta = -2 \log_N \left(\sqrt{\frac{N(1 + t_p/\tau)}{F_Q}} \right) \approx \log_N \left(\frac{F_Q}{t_p} \cdot \frac{\tau}{N} \right). \quad (\text{S23})$$

Without loss of generality, we can set $\tau = 1$ as a unit and focus on the scaling behavior of F_Q/t_p with respect to N .

Next, we exploit the established bound of the QFI growth [cf. Eq. (4) in the main text], i.e. $F_Q/N \lesssim R_L^D(t_p)$ (up to some constant coefficients) to derive the strong precision limits set by Eqs. (7-9) in the main text. For short-range interacting system, i.e. $R_L(t_p) \sim t_p$ [S3, S6], using our result in Eq. (4) of the main text, we can conclude that, in order to achieve the QFI density

of $F_Q/N \sim N^{\Delta_f}$ with the assumption that $\Delta_f \in [0, 1]$, a metrological state preparation time at least on the order of

$$t_p \sim \left(\frac{F_Q}{N} \right)^{\frac{1}{D}} \sim N^{\frac{\Delta_f}{D}}, \quad (\text{S24})$$

would be required. Hence, the metrological enhancing exponent in this scenario is given by

$$\Delta = \log_N N^{(1-\frac{1}{D})\Delta_f} = \left(1 - \frac{1}{D} \right) \Delta_f \leq 1 - \frac{1}{D}, \quad (\text{S25})$$

namely Eq. (7) in the main text. While for long-range interacting systems: (i) if $\alpha \in (2D, 2D + 1]$, the light cone is given by $R_L(t_p) \sim t_p^{1/\xi}$ [S4], and then Eq. (4) in the main text allows us to find that the minimal state preparation time to reach $F_Q/N \sim N^{\Delta_f}$ needs to satisfy

$$t_p \sim \left(\frac{F_Q}{N} \right)^{\frac{\xi}{D}} \sim N^{\frac{\xi}{D}\Delta_f}, \quad (\text{S26})$$

which further leads to Eq. (8) in the main text, i.e.

$$\Delta = \log_N \left(\frac{N^{\Delta_f}}{t_p} \right) = \left(1 - \frac{\xi}{D} \right) \Delta_f \leq 1 - \frac{\xi}{D}. \quad (\text{S27})$$

(ii) if $\alpha \in (D, 2D]$, then $R_L(t_p) \sim e^{t_p}$ [S5, S8]. Similarly, the state preparation time shall be larger than

$$t_p \sim \log N^{\Delta_f/D} \sim \text{polylog}(N), \quad (\text{S28})$$

and thus we have

$$\Delta \leq 1 - \log_N \text{polylog}(N), \quad (\text{S29})$$

namely Eq. (9) in the main text.

5. Behavior of the QFI growth of Ising model

The pure Ising model for demonstrating the metrological enhancement of long-range interacting systems is exactly solvable. Below, we provide the analytical formulas to calculate the QFI dynamics. Starting from the coherent spin state along the x direction, the maximal QFI at a given evolution time t (by optimizing the interrogation operator $S_{\hat{n}}$ that points along the direction \hat{n}) can be obtained as follows

$$F_Q(t) = N + \max_{\phi} \sum_{i \neq j} \left[\sin^2(\phi) C_{ij}^y(t) + \frac{1}{2} \sin(2\phi) C_{ij}^{yz}(t) \right], \quad (\text{S30})$$

where

$$C_{ij}^y(t) = \frac{1}{2} \prod_{k \neq i, j} \cos[2(J_{ik} - J_{jk})t] - \frac{1}{2} \prod_{k \neq i, j} \cos[2(J_{ik} + J_{jk})t], \quad (\text{S31})$$

and

$$C_{ij}^{yz}(t) = -\sin(2J_{ij}t) \left(\prod_{k \neq i, j} \cos(2J_{ik}t) + \prod_{k \neq i, j} \cos(2J_{jk}t) \right), \quad (\text{S32})$$

with $J_{ij} \equiv 4/(\mathcal{N}_{\alpha}|i-j|^{\alpha})$. For $\alpha = 0$ and $J_{ij} = 4/N$, the above formulas reduce to the well-known results for spin squeezing under one-axis-twisting quantum dynamics [S9, S10], namely

$$F_Q(t) = N + N(N-1) \left(A + \sqrt{A^2 + B^2} \right) / 4, \quad (\text{S33})$$

where $A = 1 - [\cos(2u)]^{N-2}$, and $B = 4 \sin(u) [\cos(u)]^{N-2}$ with $u = 8t/N$.

Based on these analytical formulas of the QFI at any evolution time t , the QFI dynamics for a given system size N can be determined numerically. In Fig. S1, we depict the scaling behavior of the maximal QFI by setting the value

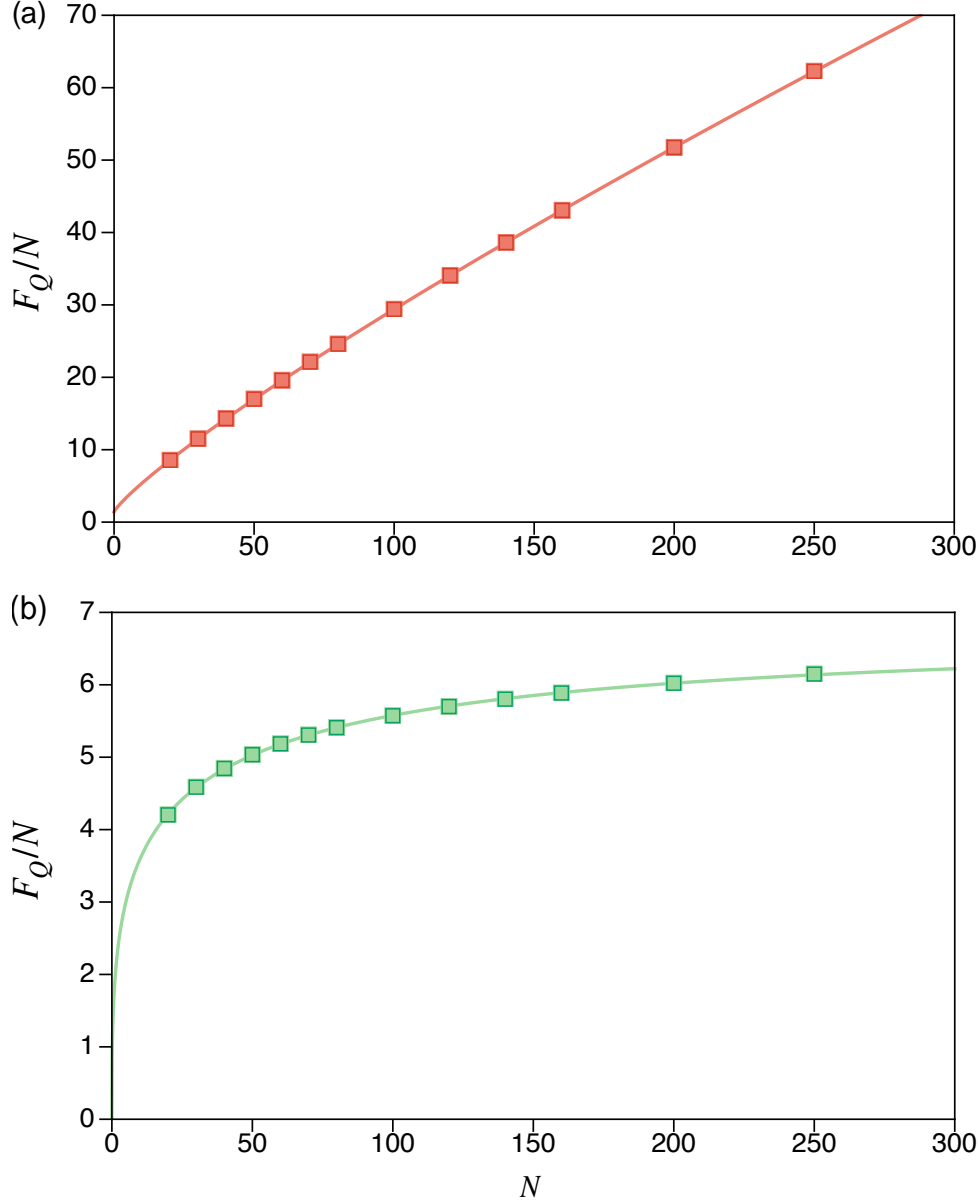


FIG. S1. **Scaling behavior of the QFI for long-range Ising chain.** Starting from the coherent spin state along the x direction, we maximize the QFI at all times t by optimizing local interrogation operators, $K_i = S_{\hat{n}}$, with $S_{\hat{n}}$ the spin-1/2 operator along the direction \hat{n} . Each square marks the optimum of F_Q for a specific value of N . **a**, Polynomial increase of the QFI at $\alpha = 0.5$ as $F_Q/N = a + bN^c$ with $a = 1.41$, $b = 0.57$ and $c = 0.85$ (red curve). **b**, Saturation of the QFI for $\alpha = 1.4$. The maximal QFI is well fitted by the green curve, i.e. of the form $F_Q/N = a[1 - e^{-(N/b)^c}]$ with $a \approx 6.65$, $b \approx 19.76$ and $c \approx 0.37$. Therefore, for large-size systems, the QFI would saturate as $F_Q \sim N$.

of the interaction decaying exponent α as 0.5 and 1.4 respectively [cf. Eq. (10) in the main text]. Importantly, our numerical result suggests that the maximal QFI for $\alpha \gtrsim 1.4$ would not surpass the SQL.

-
- [S1] Boixo, S., Flammia, S. T., Caves, C. M. & Geremia, J. Generalized limits for single-parameter quantum estimation. *Phys. Rev. Lett.* **98**, 090401 (2007).
 - [S2] Bravyi, S., Hastings, M. B. & Verstraete, F. Lieb-Robinson bounds and the generation of correlations and topological quantum order. *Phys. Rev. Lett.* **97**, 050401 (2006).
 - [S3] Lieb, E. H. & Robinson, D. W. The finite group velocity of quantum spin systems. *Commun. Math. Phys.* **28**, 251–257 (1972).
 - [S4] Tran, M. C., Guo, A. Y., Baldwin, C. L., Ehrenberg, A., Gorshkov, A. V. & Lucas, A. Lieb-Robinson light cone for power-law interactions. *Phys. Rev. Lett.* **127**, 160401 (2021).
 - [S5] Eisert, J., van den Worm, M., Manmana, S. R. & Kastner, M. Breakdown of quasilocality in long-range quantum lattice models. *Phys. Rev. Lett.* **111**, 260401 (2013).
 - [S6] Kuwahara, T. & Saito, K. Strictly linear light cones in long-range interacting systems of arbitrary dimensions. *Phys. Rev. X* **10**, 031010 (2020).
 - [S7] Braunstein, S. L. & Caves, C. M. Statistical distance and the geometry of quantum states. *Phys. Rev. Lett.* **72**, 3439–3443 (1994).
 - [S8] Hastings, M. B. & Koma, T. Spectral gap and exponential decay of correlations. *Commun. Math. Phys.* **265**, 781–804 (2006).
 - [S9] Kitagawa, M. & Ueda, M. Squeezed spin states. *Phys. Rev. A* **47**, 5138–5143 (1993).
 - [S10] Pezzè, L., Smerzi, A., Oberthaler, M. K., Schmied, R. & Treutlein, P. Quantum metrology with nonclassical states of atomic ensembles. *Rev. Mod. Phys.* **90**, 035005 (2018).